Article

Synthesis of a Novel Co-B/CTAB Catalyst *via* Solid-state-reaction at Room Temperature for Hydrolysis of Ammonia-borane

HU Haibin[1], LONG Bo[1,2,3], JIANG Yifan[1], SUN Shichang[1], Ibrahim LAWAN[1], ZHOU Weiming[1,3], ZHANG Mingxin[1], WANG Liwei[4*], ZHANG Fan[5*] and YUAN Zhanhui[1*]

1. College of Materials Engineering, Fujian Agriculture and Forestry University, Fuzhou 350002, P. R. China;

2. College of Mechanical and Electrical Engineering, Fujian Agriculture and Forestry University, Fuzhou 350002, P. R. China;

3. Key Laboratory of National Forestry & Grassland Bureau for Plant Fiber Functional Materials, Fujian Agriculture and Forestry University, Fuzhou 350002, P. R. China;

4. Ocean College, Minjiang University, Fuzhou 350108, P. R. China;

5. School of Chemistry and Chemical Engineering, Shanghai Jiao Tong University, Shanghai 200240, P. R. China

Abstract Cobalt-boride(Co-B) is emerging as one of the promising materials in the base-hydrolytic dehydrogenation of ammonia-borane(AB). In order to avoid the low specific area and poor catalytic capacity of Co-B catalyst caused by aggregation arising from the strong reducing property and rapid reaction condensation of sodium borohydride($NaBH_4$), novel cobalt boride/cetyltrimethylammonium bromide(Co-B/CTAB) catalyst was obtained *via* solid-state grinding at room temperature, and the catalyst was further characterized by XRD, SEM, XPS and BET. The hydrogen generation rate(HGR) was then determined by the hydrolysis reaction of AB. The SEM images indicate that a lot of irregular folds and curled edges are formed on the sample with a maximum surface area of 145.57 m^2/g, thus possibly resulting in the high hydrogen production(HGR was 10.68 $L\cdot min^{-1}\cdot g^{-1}$), which may be attributed to CTAB that provide favorable large specific surface area and abundant porous structure. Additionally, catalyst will not be affected by solvants during solid-state reaction. As a diluent, the surfactant CTAB hindered the reaction rate of sodium borohydride reduction to cobalt boride and obtained the novel catalyst with a large specific surface area.

Keywords Hydrogen generation rate; Ammonia borane; Co-B; Solid-state reaction

1 Introduction

With the increasingly prominent energy demands and environmental issues, clean and sustainable energy has become a research hotspot[1,2]. As a kind of clean energy, hydrogen energy has been paid much attention by researchers[3,4], which can be produced by water, biomass, and its affiliated chemical products, such as fossil fuel[5,6]. And borohydride(ammonia-borane, hydrazine-borane and sodium borohydride, etc.) plays an important role in the base-hydrolytic dehydrogenation. Among these borohydride, ammonia-borane(AB) has been considered as a promising option because of its higher hydrogen contents(19.6%, mass ratio), high solubility(336 g/L in water), and appreciable stability at room temperature[7,8]. Normally, the stored hydrogen of NH_3BH_3 is released by a hydrolysis reaction[9,10].

$$NH_3BH_3(s)+2H_2O(l) \longleftrightarrow NH_4BO_2(l)+3H_2(g) \quad (1)$$

Theoretically, 1 mol of ammonia-borane can produce 3 mol of hydrogen by hydrolyzing and decomposing BH_3 group and NH_3 moiety, as shown in above reaction. It can be interpreted as the initial hydrogen production of 8.9%(mass ratio) for NH_3BH_3 and water[11,12]. In addition, one of the most important factors affecting the hydrolysis reaction is the presence of the hydrolysis catalyst. Precious metals, such as platinum, palladium, and rhodium are generally considered to be highly active hydrolysis catalysts[7]. Nevertheless, the application of precious metal was limited by its high cost and short catalytic lifetime. In 2006, Xu *et al*.[13] firstly pointed out that transition metals are active in the hydrolysis of AB, and this viewpoint has attracted widespread attention of researchers. Transition metals not only exhibit excellent catalytic

*Corresponding authors. Email: zhanhuiyuan@fafu.edu.cn; wlw@mju.edu.cn; fan-zhang@sjtu.edu.cn

Received June 26, 2020; accepted September 1, 2020.

Supported by the International Funding of Fujian Agriculture and Forestry University, China(No.KXB16001A), the Project of the Department of Science and Technology of Fujian Province, China(No.2017H6003) and the Open Project Program of Key Laboratory of National Forestry & Grassland Bureau for Plant Fiber Functional Materials, China(Nos.2019KFJJ17, 2019KFJJ15).

performance, but also have lower price than precious metals[14]. According to previous studies, cobalt boride is a catalyst for ammonia borane with an appreciable catalytic capacity in view of the electron-deficient property of boron[15]. However, the pre-obtained Co-B exhibits some negative features(lower surface area, homogeneity of its particle, and inferior thermal stability) that results in lower catalytic performance on the hydrolysis of AB[16]. Therefore, it is necessary to improve the catalytic capacity of cobalt boride. Fernandes *et al*.[17] synthesized Co-Ni-B by chemical reduction and found that the activity of the catalyst can be significantly improved by adding Ni. Shi *et al*.[18,19] proposed that carbon nano-tubes and r-graphene accelerators could increase the surface area, enhance the catalytic performance and achieve the dispersion of Co-B. Wang *et al*.[20] synthesized a kind of urea modified flocculent cobalt boride by controlling its morphology. Therefore, controlling the morphology of Co-B is of great significance to improve its surface area. Surfactant is commonly employed as an additive to synthesize nanoparticles and nanostructured materials, acting as either a template or a shape directing agent[21]. Gupta *et al*.[22] synthesized mesoporous cobalt-boride using nonionic surfactants.

On the other hand, the catalytic efficiency of catalysts is affected by the synthesis method. Different catalytic performance is achieved by different synthesis methods. The specific surface area of cobalt boride prepared by liquid phase reaction is small due to the solvation of the solution. The production of Co-B, at low or even room temperature by solid-state reaction, has obvious features, such as simple and convenient, less solvent and reduced contamination, and high yield product[23]. Based on these advantages, this synthesis method has always been favored by researchers. However, as a way of producing Co-B with a large surface area, solid-state reaction at present is enormous challenges ahead to prepare Co-B catalyst[24,25].

In order to avoid the low specific surface area and poor catalytic capacity of Co-B catalyst caused by aggregation, cetyltrimethylammonium bromide(CTAB), one kind of surfactant as a template and a shape directing agent, was first used here to control solid phase reaction and prepare a novel brain-like gully catalyst at room temperature *via* solid-state reaction. The BET value is about 5 times as large as that of Co-B prepared by a traditional solid-state reaction. The agglomeration of the Co-B catalyst in the hydrolysis of ammonia borane has been significantly reduced by CTAB. Besides, catalyst will not be affected by CTAB during solid-state reaction. Co-B/CTAB thus becomes a promising catalyst in the hydrolysis of ammonia borane for hydrogen production in the industrial application because of its excellent catalytic performance.

2 Experimental

2.1 Materials

Cobalt(II) chloride hexahedron($CoCl_2·6H_2O$, 99.9%), ammonia-borane complex(AB, 97%), sodium borohydride ($NaBH_4$, 98%), and cetyltrimethylammonium bromide (CTAB, 99.0%) were purchased from Alfa Aesar, Fuchen Chemical Reagent Co., Ltd.(Tianjin, China), and Hedong District Reagent Factory of Tianjin, China, respectively. And they were all the analytical grade purity without further purified.

2.2 Synthesis of the Catalysts

The catalysts were synthesized according to the procedure previously reported in the literature[23]. The procedure is described in Fig.1, where 1 mmol of $CoCl_2·6H_2O$ and 5 mmol CTAB were mixed by grinding in a gate mortar till the mixture turned pale blue[Fig.1(A)]. The $NaBH_4$ powders(0.05 mol) were then evenly sprinkled over the mixture and continued to grind. The sample turned into black, which was then rinsed with distilled water and anhydrous ethanol several times to obtain clean samples(Fig.1). The obtained samples further were stirred before drying in a vacuum oven at 60 °C for 24 h and the final sample(65 mg) was denoted as Co-B/CTAB. Acting as reference, a sample was also prepared with $CoCl_2·6H_2O$ and $NaBH_4$ using the aforementioned procedure, and it was denoted as Co-B.

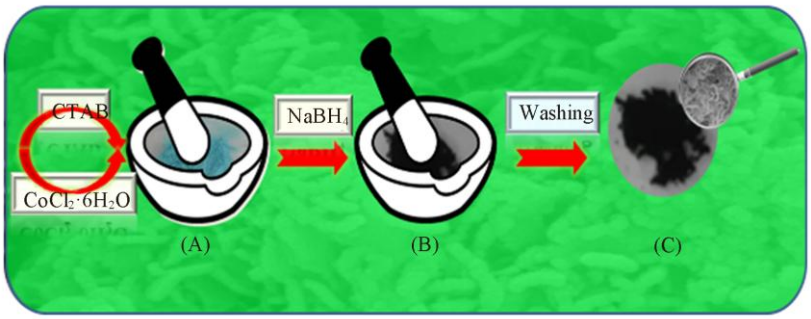

Fig.1 Schematic diagram of preparation and synthesis of catalyst
(A) $CoCl_2·6H_2O$/CTAB; (B) Co-B/CTAB and $CoCl_2·6H_2O$/CTAB; (C) Co-B/CTAB.

2.3 Characterization of the Catalysts

XRD patterns of the catalysts were obtained at a 2θ range of 10°—80° with a scan rate of 1°/min on a Rigaku D/max 2500 X-ray diffractometer(Cu $K\alpha$, λ=0.154178 nm). The samples were analyzed by SEM at 40 kV and 40 mA, respectively, while specific surface area was determined by BET using the Quanta chrome autosorb-1 volumetric analyzer. And X-ray photoelectron spectrometer(XPS) was used for testing the composition and structure. Among them, the vacuum degree of the room, where the samples were analyzed was 5×10^{-10} Pa, with Al $K\alpha$ ray($h\nu$=1253.6 eV) served as an excitation source,

working voltage being 15 kV, filament current being 10 mA and the charge being corrected at C_{1s}=284.80 eV.

2.4 Measurement of Hydrogen Generation Rate (HGR)

The hydrogen generation reaction of NH_3BH_3 was performed in a 50 mL single-neck glass flask reactor using a water bath heating system[23]. About 0.0050 to 0.20 g of each catalyst was put into the reactor along with a solution containing NH_3BH_3 and NaOH. The hydrolytic dehydrogenation of NH_3BH_3 occurred in an ultrasonoscope with a circulating water bath, and the reaction was conducted at controlled temperature. The volume of hydrogen generation throughout the entire process was tested with a water-filled gas burette. The effect of reaction temperature on the hydrolysis of NH_3BH_3 was also studied, and the range of temperature for reaction was 25—40 °C.

3 Results and Discussion

3.1 Structure of the Pre-catalyst

The XRD patterns of Co-B and Co-B/CTAB are shown in Fig.2(A), which indicate that the structures of the catalysts are slightly different. In Fig2(A), all the samples exhibit a broad peak at 2θ=45°, implying mixed crystals and amorphous phase[26]. Additionally, both samples kept magnetic and could be easily removed from the solution by a magnet after reaction.

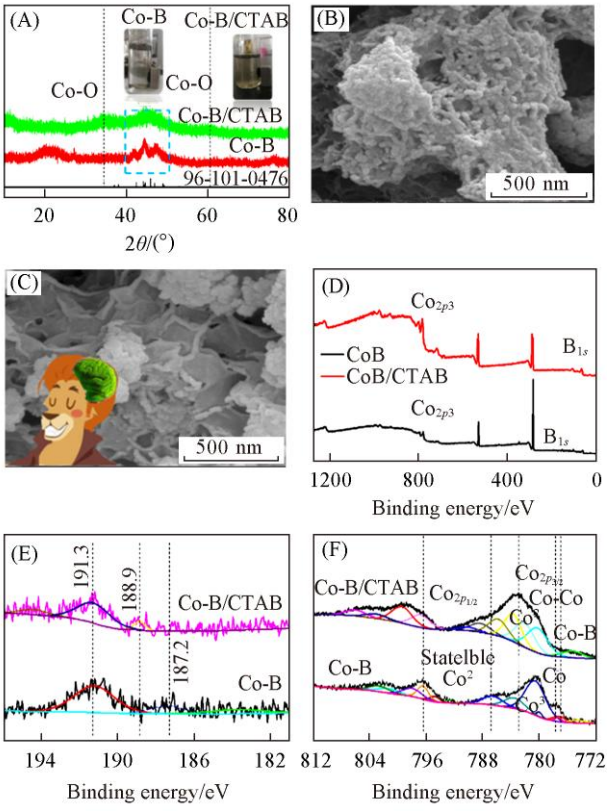

Fig.2 XRD spectra of Co-B and Co-B/CTAB(A), SEM images of Co-B(B) and Co-B/CTAB(C), XPS survey spectra(D), the B_{1s}(E) and the Co_{2p}(F) peak level for the Co-B and Co-B/CTAB samples

It further showed that the typical amorphous nature of the Co-B/CTAB catalysts with surface defects due to incomplete-crystal phase enhanced the catalytic activity[24,27]. Furthermore, the magnetic property of the modified catalyst by CTAB also kept magnet, which was easily recycled. The molar ratio of Co:B was analyzed by ICP-OES, which is 1:0.30 for Co-B/CTAB and 1:0.33 for Co-B, respectively. The results of ICP-OES are consistent with the XRD result[23]. The SEM images of Co-B and Co-B/CTAB catalysts are shown in Fig.2(B) and (C), respectively. As shown in Fig.2(B), Co-B is characterized by a lot of regular spherical nanoparticles. In contrast, Fig.2(C) shows that Co-B/CTAB has more irregular folds and curled edges. The significant morphological differences between the two samples indicate that morphology may be affected by the synthetic routes. CTAB is commonly used as a template for synthesizing intermediate nanoparticles shape directing agent. The structure of the intermediate product can be maintained by Co-B/CTAB that is formed by reducing sodium borohydride[28,29]. Subsequently, the surface compositions and electronic interaction structure between Co and B atoms in samples were analyzed by XPS [Fig.2(D)—(F)]. For the high-resolution B_{1s} spectra of the samples, there were distinct peaks with binding energy intensities of 191.3 and 188.9 eV, indicating that there is oxidized borate on the surface of the two pre-samples[18,30,31]. For the Co_{2p} level as shown in Fig.2(F), it is shown that the XPS spectra of Co_{2p} spectra($Co_{2p_{3/2}}$ and $Co_{2p_{1/2}}$) are two types of spin-orbital states. The observed peaks indicate that Co species, at binding energies of 780.9 and 782.6 eV, exist in metallic(Co^0) and oxidized (Co^{2+}) states, respectively, while a satellite peak at around 787.0 eV forms high-resolution XPS spectra of Co_{2p} of Co-B[32,33]. According to the Co_{2p} spectrum of Co-B/CTAB, the peaks at binding energies of 780 and 782 eV correspond to Co^0 and Co^{2+} species [18,30]. As shown in Fig.2(F), the peak with a lower binding energy of 777.0 eV was formed during the interaction between Co^0 and B due to the reverse electron-transfer from B to Co atom. Co^{2+} species(CoO) are detected in the as-prepared Co-B and Co-B/CTAB samples, indicating that Co or Co-B surfaces were spontaneous oxidized in both cases[34].

Nitrogen adsorption-desorption isotherms(ADI) of the pre-samples are shown in Fig.3. It can be seen from the output that the isotherms are similar to type IV ADI with a hysteresis loop as per IUPAC classification. The porosities of the Co-B and Co-B/CTAB catalysts were also calculated by N_2 ADI

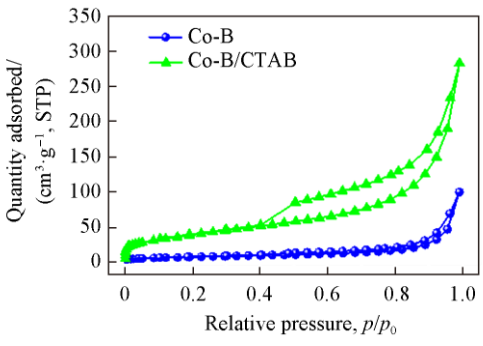

Fig.3 N_2 adsorption-desorption isotherms of Co-B and Co-B/CTAB

(Fig.3). Therefore, the hysteresis loop under the relative pressure(p/p_0) ranging from 0.40 to 0.95 is observed in the isotherm of Co-B/CTAB, which can be attributed to the porosity of Co-B/CTAB. The Co-B sample exhibits lower N_2 adsorption pore volume, while the Co-B/CTAB samples exhibit superior pore and mesoporous volumes. The surface areas of Co-B and Co-B/CTAB are 29.17 and 145.57 m^2/g, respectively (Table 1), revealing that an enhanced porous structure is achieved with Co-B/CTAB when compared with the control sample(Co-B). The BET surface area of Co-B/CTAB achieved was also compared with the established results of Co-B in the literatures(224.1 m^2/g)[23], Catkin-like Co-B(224.7 m^2/g)[35] and Co-B/CTAB(114.1 m^2/g)[27], further confirming that significant improvement has been achieved in terms of porosity. The specific surface area is one of the factors that could affect the hydrolytic rate of ammonia borane[16]. Thus, the specific surface area is not proportional to the hydrolytic rate of ammonia borane.

Table 1 Physical-chemical properties of pre-samples

Catalyst	BET surface area/($m^2 \cdot g^{-1}$)	Average pore diameter[a]/nm	Pore volume[b]/($cm^3 \cdot g^{-1}$)
Co-B/CTAB	145.57	7.62	0.44
Co-B	29.17	8.70	0.08

a. Average pore width for adsorption(4 V/A by BET); *b*. the volume of pores for BJH adsorption between 1.7 and 300 nm in diameter.

3.2 HGR of the Catalysts

The catalytic activities of the catalysts in the hydrolysis reaction of NH_3BH_3 are presented in Fig.4. According to Fig.4, the HGR of AB using Co-B/CTAB increases as time advances. The HGR of AB using the catalyst can be up to 106.8 mL/min and the transformation rate can be up to 10.68 $L \cdot min^{-1} \cdot g^{-1}$ for hydrolysis reaction in an ultrasonic bath(Fig.4). However, the HGR values of AB in the presence of Co-B/CTAB catalyst under different bath conditions are shown in Fig.4(A). The HGR of AB using the Co-B/CTAB(redefined Co-B/$CTAB_n$) catalyst can only reach 96.67 mL/min with a transformation rate of *ca*. 9.67 $L \cdot min^{-1} \cdot g^{-1}$ for the hydrolysis reaction in a water bath heating system. Therefore, it can be concluded that ultrasound facilitates the elimination of dispersion between particles and increased the charge diffusion rate between reaction substances, which can further improve the reaction efficiency. Thus, the subsequent hydrolysis reactions were performed under ultrasonic conditions. Ultrasound prevents Co-B/CTAB catalyst from agglomeration caused by exothermic heat during reaction, increases contact area between reactants and improves catalytic performance[36]. Similarly, hydrogen generation using Co-B increases with time(Fig.4). Besides, the HGR of the Co-B samples were from 40.05 mL/min to 85.6 mL/min and transformation rate can be increased from 4.00 $L \cdot min^{-1} \cdot g^{-1}$ to 8.56 $L \cdot min^{-1} \cdot g^{-1}$ respectively, indicating that Co-B/CTAB exhibits higher catalytic activity than Co-B in the hydrolysis of NH_3BH_3. In addition, Co-B/CTAB catalysts demonstrate a typical amorphous nature, as shown in XRD and XPS and it is possibly attributed to surface defects due to the incomplete crystal phase. It is said that the prepared Co-B/CTAB is one of the most energetic noble-metal-free catalysts because of its superior transformation rate in the hydrolysis of NH_3BH_3 (Table 2). The transformation rates of the Co-B/CTAB catalysts are superior to that of Co-B catalyst reported in previous researches[Co-B(9.16 $L \cdot min^{-1} \cdot g^{-1}$)][37]. Till today, the transformation rate of honeycomb-like Co-B is 6.9 $L \cdot min^{-1} \cdot g^{-1}$[23] and that of Co-B/CTAB is 2.2 $L \cdot min^{-1} \cdot g^{-1}$[27]. The catalytic hydrogen production performances of different catalysts are given in Table 2. The hydrolysis rate is affected by the specific surface area and the activity of the catalyst during hydrolysis reaction.

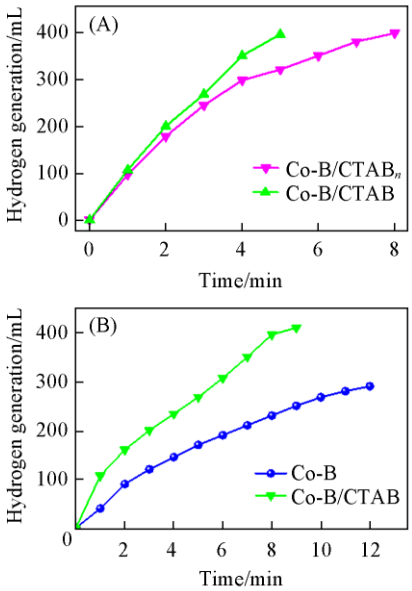

Fig.4 HGR of AB in the presence of Co-B/CTAB catalyst under different bath conditions(A) and HGR of AB in the presence of the Co-B and Co-B/CTAB catalysts at 30 °C in an ultrasonic bath(B)

3.2.1 Effect of Catalyst Concentration on HGR

Similarly, it is known that HGR also depends on the hydrolytic concentrations of catalyst, as manifested in this study. The HGR of AB in the Co-B/CTAB catalysts at different concentrations has been recorded(Fig.5). According to Fig.5, an increase in the hydrolytic concentration of catalyst in the reaction at 30 °C has resulted in an increase in the HGR of Co-B from 28.5 mL/min at 5 mg of catalyst to 59.3 mL/min at 20 mg of catalyst[Fig.5(A)]. However, the HGR in the presence of Co-B/CTAB increases from 53.6 mL/min with 5 mg of catalyst to 196.2 mL/min at 20 mg of catalyst[Fig.5(B)]. With the increase of catalyst concentration, hydrogen production increases. However, there was no significant difference in HGR when 5 mg and 10 mg of Co-B were used. When 20 mg of Co-B was added, the produced hydrogen was apparently increased. For the case of Co-B/CTAB, the rate of hydrogen production increases as catalyst increases[38,39] due to that the agglomeration of the Co-B catalyst in the hydrolysis of ammonia borane has been reduced by CTAB.

3.2.2 Effect of NH_3BH_3 Concentration on HGR

As is known to all, the HGR predominantly depends on the hydrolytic concentration of NH_3BH_3. The HGR with the Co-B and Co-B/CTAB catalysts at different concentrations of

NH_3BH_3 is illustrated in Fig.6. In Fig.6, an increase in the hydrolytic concentration of AB at 30 °C has resulted in an increase in the HGR of the Co-B from 55.8 mL/min with 0.05 mol of NH_3BH_3 to 66.5 mL/min with 0.15 mol of NH_3BH_3 [Fig.6(A)]. The HGR in the presence of Co-B increases from 88.12 mL/min with 0.05 mol of NH_3BH_3 to 106.3 mL/min with 1.0 mol of NH_3BH_3[Fig.6(B)]. As the concentration of reactants in NH_3BH_3 increases, the HGR increases slightly, while as time advances, the reaction rate gradually slows down, which is caused by the decrease of concentration of NH_3BH_3 reaction system[40,41]. In this study, 0.05 mol of NH_3BH_3 was used to test the catalytic activity of the Co-B and Co-B/CTAB catalysts.

Table 2 Comparison of HGR, durability and activation energy of some similar catalysts reported in the literature

Catalyst used	Hydrogen generation measurement	HGR/ ($L \cdot min^{-1} \cdot g^{-1}$ catalyst)	Durability	Activation energy/ ($kJ \cdot mol^{-1}$)	BET surface area/ ($m^2 \cdot g^{-1}$)	Reference
Co-B	2.7 mmol of $NaBH_4$ and 2.5 mmol of NaOH as 1%(mass ratio) 10 mg of catalyst	5.31	79.3% after 5 cycles	30	82.1	[20]
Co-B	0.12 mol/L NH_3BH_3, 10 mg of catalyst	9.16	90% after 4cycles	47.5	/*	[42]
Co-B/glass	0.025 mol/L AB/SBH, molar ratio kept constant at 9:1	8.2—13	Lower rate(about 6 times)	33.9	/*	[43]
Co-B/Cu sheet	1%(mass ratio) $NaBH_4$ with 5% (mass ratio) NaOH	5.50	79.1% catalytic activity after 5 cycles	37.8	/*	[44]
Co-W-B/foam sponge	NH_3BH_3	3.33	78.4% of their initial catalytic activity even after 5 cycles	32.2	/*	[45]
Co-W-B	6 mol/L KOH solution	/*	89.2% of its initial capacitance after 2500 cycles	/*	169.2	[46]
Co-Mo-B	5%(mass ratio) $NaBH_4$+ *x*%(mass ratio) NaOH	1.30	75.1% catalytic activity of its initial activity after 3 cycles	51.0	45.6	[47]
Co-Cu-B	2.5%(mass ratio) $NaBH_4$ 5% NaOH	4.97	/*	17.38	/*	[48]
Co-Ce-B/TiO_2	$NaBH_4$ and NaOH	4.56	/*	29.51	/*	[49]
Co-Co_2B/Ni-Ni_3B	0.019 g of $NaBH_4$ in 2.5 mL of 0.025 mol/L NaOH solution	4.30	/*	35.245	/*	[50]
Co-Mo-B/Ni foam	40 mg of NH_3BH_3	5.30	/*	45.5	/*	[51]
Co-Mo-Pd-B	NaOH and $NaBH_4$	6.02	/*	36.36	/*	[52]
Fe-Co-B/Ni foam	15%(mass ratio) $NaBH_4$ and 5%(mass ratio) NaOH	22.0	/*	27	/*	[53]
Co-La-Zr-B	5%(mass ratio) $NaBH_4$ and 2%(mass ratio) NaOH	0.01415	75% catalytic activity of its initial activity after 3 cycles	51.24	143	[54]
Co-B/CTAB		**10.68**	/*	**14.9**	**145.6**	**This work**

*Not reported or no detailed data are available.

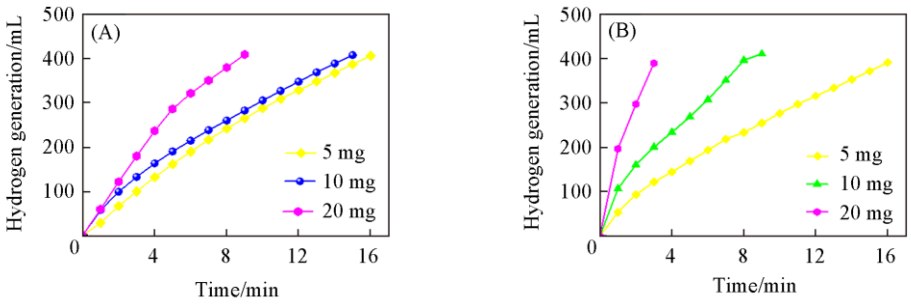

Fig.5 HGR at different concentrations of Co-B(A) and Co-B/CTAB(B) at 30 °C in an ultrasonic bath

3.2.3 *Effect of Temperature on HGR*

According to Arrhenius formula[35]:

$$\ln K = -(E_a/RT) + \ln A \quad (2)$$

where k, E_a, A, R and T are the rate constant of hydrolysis reaction, activation energy, factor before index, molar gas constant and thermodynamic temperature, respectively. The apparent activation energy(E_a) in the hydrolysis of NH_3BH_3 was calculated based on the values of the rate constants recorded at different temperatures. The HGR using the Co-B/CTAB catalyst can be up to 106.8 mL/min. The results indicate that HGR mainly depends on the hydrolytic temperature of AB. The HGR in the Co-B and Co-B/CTAB catalysts at different hydrolysis

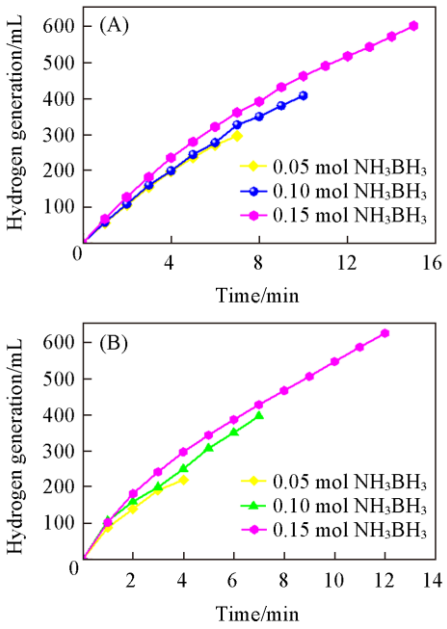

Fig.6 HGR at different concentrations of AB at 30 °C for Co-B(A) and Co-B/CTAB(B) in an ultrasonic bath

temperatures is illustrated in Fig.7. As can be seen from Fig.7, there is an increase when the reaction temperature increases from 25 °C to 40 °C, resulting in an increase in the hydrogen generation within the limits of the temperature used in the study. In the presence of Co-B, HGR significantly increases from 56.3 mL/min to 94.5 mL/min at 25—40 °C[Fig.7(A)], while that in the presence of Co-B/ CTAB increases from 90.4 mL/min to 125.8 mL/min at 25—40 °C[Fig.7(B)]. The result shows that the HGR of AB increases gradually as hydrolysis temperature increases, so temperature is one of the important factors affecting the hydrolysis rate of ammonia borane[20,23,40].

The logarithm of rate constants against the reciprocal of corresponding hydrolysis reaction temperatures is presented in Fig.7(C). In view of the slope of the fitting line in Fig.7(C), the E_a values for the hydrolysis of AB in the presence of the samples(Co-B and Co-B/CTAB) are calculated to be 29.91 and 14.56 kJ/mol in Fig.7(C), respectively. The relatively lower E_a of the Co-B/CTAB catalyst indicates that its catalytic activity is higher than that of the Co-B catalyst. In other words, the E_a value of the Co-B/CTAB catalyst is lower than those of many other Co-B alloy catalysts, such as Co-B(30 kJ/mol)[23], Co-B(47.5 kJ/mol)[37] and Co-B hollow spindle(26.2 kJ/mol)[19]. The activation energy of different catalysts is listed in Table 2. As mentioned earlier, the Co-B/CTAB catalyst exhibits superior activity in the NH_3BH_3 hydrolysis. The HGR results reveal that the Co-B/CTAB catalyst is characterized by not only appreciable BET surface area but also superior mesopores. Such special structure can affect catalytic activity because of the change in surface area. Furthermore, BET and SEM showed that the superior catalytic activity of Co-B/CTAB could obtain the high surface area and superior porous structure. XPS result indicates that its superior catalytic performance has been obtained during the interaction between Co^0 and boron due to the reverse electron-transfer from B atom to Co atom. The increase in specific surface area leads to more catalytic activity and higher catalytic performance of the Co-B/CTAB catalyst[20,40].

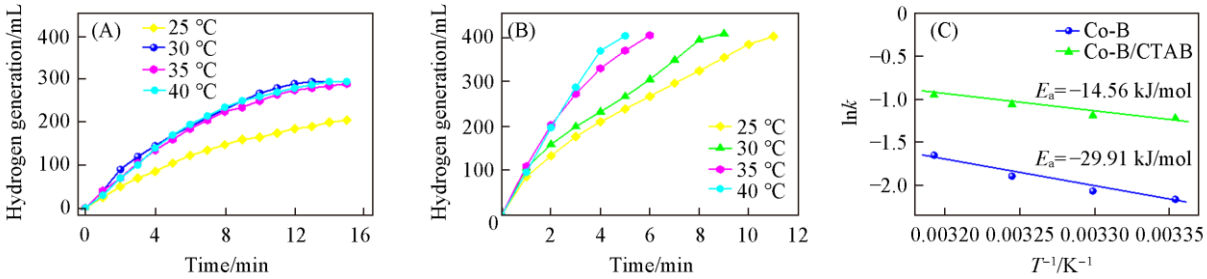

Fig.7 HGR of Co-B(A) and Co-B/CTAB(B) at different hydrolysis reaction temperatures and the activation energy at 25—40 °C in an ultrasonic bath(C)

3.2.4 Effect of NaOH Concentration on HGR

It has been shown that the HGR depends on the hydrolytic concentration of NaOH in Fig.8. According to Fig.8, increase in the hydrolytic concentration of NaOH in the reaction at 30 °C has resulted in an increase in the HGR of Co-B from 40.6 mL/min to 69.1 mL/min[Fig.8(A)]. In contrast, the HGR of the Co-B/CTAB catalyst increases from 49.6 mL/min to 106.3 mL/min when the hydrolytic concentration of NaOH increases from 1% to 10%(mass ratio)[Fig.8(B)]. Thus, the alkaline concentration in the hydrolysis reaction is also one of

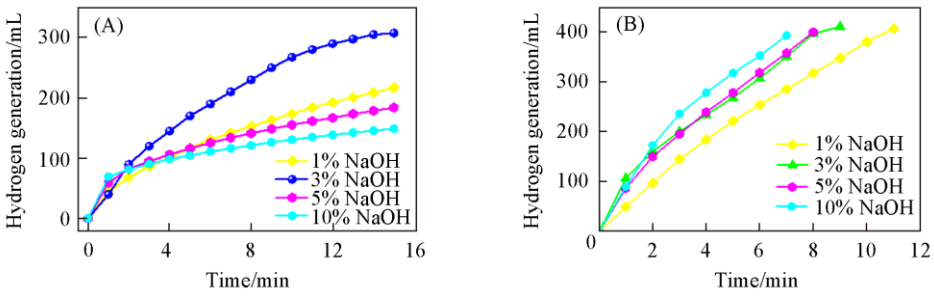

Fig.8 Effects of NaOH concentration on the hydrogen generation rate at 30 °C for Co-B(A) and Co-B/CTAB(B) in an ultrasonic bath

the crucial factors affecting the catalytic efficiency of the catalysts. To sum up, the concentration of sodium hydroxide affects the hydrolysis rate of ammonia borane and the activity of catalyst[55]. The speed, at which H_2O molecules and NH_3BH_3 reach the catalyst surface is affected by the concentrations of sodium hydroxide(NaOH)[23,36].

Furthermore, the catalytic hydrolysis mechanism of AB by Co-B catalyst was studied and the novel Co-B/CTAB catalyst was synthesized in the present study using surfactant as a template(Fig.9). Moreover, as can be seen from BET results, the specific surface area increased by nearly 5 times when compared with that of Co-B. The SEM images also indicate that more irregular multi-layer nano-sheets were generated because the surfactant(CTAB) prevented the morphology of Co-B booster from forming as a shape directing agent. CTAB could provide favorable structure support for Co-B/CTAB after it reduced by sodium borohydride. The XRD results also indicate the typical amorphous nature of the Co-B/CTAB catalysts with surface defects due to the incomplete crystal phase. As a template, the surfactant CTAB hindered the reaction rate of sodium borohydride reduction to cobalt boride and obtained a catalyst with a large specific surface area. The features could enhance the catalytic activity and prevent the Co-B/CTAB catalyst from agglomerating caused by exothermic heat during the reaction, thus further increasing the contact area of reactants, improving catalytic performance, thus further enhancing the catalytic hydrogen release capacity.

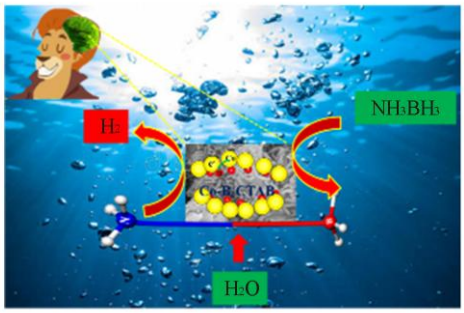

Fig.9 Illustrations of the Co-B catalytic hydrolysis mechanism of AB

4 Conclusions

The novel Co-B/CTAB has been synthesized at room temperature, which was composed of numerous small nano-sheets generated by grinding through solid-state reaction. The prepared Co-B/CTAB is characterized by a surface with abundant irregular folds and curled edges. According to the BET analysis, the surface areas of the Co-B and Co-B/CTAB catalysts could be up to 29.17 and 145.57 m^2/g, respectively, which may be attributed to that CTAB can provide favorable large specific surface area and porous structure. The synthesized catalyst(Co-B/CTAB) is utilized in the hydrolysis of NH_3BH_3 to achieve a transformation rate of 10.68 $L \cdot min^{-1} \cdot g^{-1}$ for hydrogen generation, which is significantly higher than that of the pre-modified Co-B catalyst recently reported[27]. In addition, the catalyst exhibits high catalytic activity and appreciable recoverability by a magnetic after reaction, and it can solve the problem of secondary pollution caused by the unrecyclable nano materials, indicating that it can be sustainably applied in the hydrolysis of NH_3BH_3. And it is concluded that Co-B/CTAB is a promising catalyst in the hydrolysis of ammonia borane for hydrogen production in the industrial application.

References

[1] Sun F., Wang G., Ding Y., Wang C., Yuan B., Lin Y., *Adv. Energy Mater.,* **2018**, *8*, 1800584
[2] Li J., Zhou Q., Zhong C., Li S., Shen Z., Pu J., Liu J., Zhou Y., Zhang H., Ma H., *ACS Catalysis*, **2019**, *9*, 3878
[3] Masa J., Piontek S., Wilde P., Antoni H., Eckhard T., Chen Y., Muhler M., Apfel U., Schuhmann W., *Advanced Energy Materials*, **2019**, 1900796
[4] Wei Z., Liu Y., Peng Z., Song H., Liu Z., Liu B., Li B., Yang B., Lu S., *ACS Sustainable Chemistry and Engineering*, **2019**, *7*, 7014
[5] Long B., Yang H., Li M., Balogun M. S., Mai W., Ouyang G., Tong Y., Tsiakaras P., Song S., *Applied Catalysis B: Environmental*, **2019**, *243*, 365
[6] Wang Y., Vogel A., Sachs M., Sprick R. S., Wilbraham L., Moniz S. J. A., Godin R., Zwijnenburg M. A., Durrant J. R., Cooper A. I., Tang J., *Nat. Energy*, **2019**, *4*, 746
[7] Yüksel A. C., Gülbay S. K., Ozgur C. C., *Int. J. Hydrogen Energy*, **2019**, *45*, 3414
[8] Yang X., Li Q., Li L., Lin J., Yang X., Yu C., Liu Z., Fang Y., Huang Y., Tang C., *Journal of Power Sources*, **2019**, *431*, 135
[9] Liu Y., Zhang Z., Fang Y., Liu B., Huang J., Miao F., Bao Y., Dong B., *Applied Catalysis B: Environmental*, **2019**, *252*, 164
[10] Du R., Jin X., Hübner R., Fan X., Hu Y., Eychmüller A., *Advanced Energy Materials*, **2019**, 1901945
[11] Echeverri A., Cárdenas C., Calatayud M., Hadad C. Z., Gomez T., *Surf. Sci.*, **2019**, *680*, 95
[12] Özhava D., Özkar S., *Appl. Catal. B Environ.*, **2018**, *237*, 1012
[13] Xu Q., Chandra M., *J. Power Sources*, **2006**, *163*, 364
[14] Chandra M., Xu Q., *J. Power Sources*, **2007**, *168*, 135
[15] Huang Y., Wang Y., Zhao R., Shen P. K., Wei Z., *Int. J. Hydrogen Energy*, **2008**, *33*, 7110
[16] Krishnan P., Advani S. G., Prasad A. K., *Appl. Catal. B Environ.*, **2009**, *86*, 137
[17] Patel N., Fernandes R., Guella G., Miotello A., *Applied Catalysis B: Environmental*, **2010**, *95*, 137
[18] Shi L., Chen Z., Jian Z., Guo F., Gao C., *Int. J. Hydrogen Energy*, **2019**, *44*, 19868
[19] Shi L., Xie W., Jian Z., Liao X., Wang Y., *Int. J. Hydrogen Energy*, **2019**, *44*, 17954
[20] Wang X., Liao J., Li H., Wang H., Wang R., *Int. J. Hydrogen Energy*, **2017**, *42*, 6646
[21] Llombart P., Palafox M. A., MacDowell L. G., Noya E. G., *Colloids Surfaces A*: *Physicochem. Eng. Asp*, **2019**, *580*, 123730
[22] Gupta S., Patel N., Fernandes R., Kothari D., Miotello A. C., *Int. J. Hydrogen Energy*, **2013**, *38*(34), 14685
[23] Wang X., Liao J., Li H., Wang H., Wang R., *Journal of Colloid and Interface Science*, **2016**, *475*, 149
[24] Baiker A., *Faraday Discuss. Chem. Soc.*, **1989**, *87*, 239
[25] Metin Ö., Özkar S., *Energy and Fuels*, **2009**, *23*(7), 3517
[26] Nsanzimana J. M. V., Gong L., Dangol R., Reddu V., Jose V., Xia B. Y., Yan Q., Lee J. M., Wang X., *Advanced Energy Materials*, **2019**, 1901503

[27] Gupta S., Patel N., Fernandes R., Kothari D. C., Miotello A., *Int. J. Hydrogen Energy*, **2013**, *38*, 14685
[28] Wu S. H., Chen D. H., *J. Colloid Interface Sci.*, **2004**, *273*(1), 165
[29] Gao J., Bender C. M., Murphy C., *J. Langmuir*, **2003**, *19*(21), 9065
[30] Cui Z., Guo Y., Ma J., *Int. J. Hydrogen Energy*, **2016**, *41*(3), 1592
[31] Gupta S., Patel N., Miotello A., Kothari D. C., *J. Power Sources*, **2015**, *279*, 620
[32] Lu W., Liu T., Xie L., Tang C., Liu D., Hao S., Qu F., Du G., Ma Y., Asiri A. M., Sun X., *Small*, **2017**, *13*(32), 1
[33] Jiang J., Wang M., Yan W., Liu X., Liu J., Yang J., Sun L., *Nano Energy* **2017**, *38*, 175
[34] Jiang B., Song H., Kang Y., Wang S., Wang Q., Zhou X., *Chemical Science*, **2020**, *11*, 791
[35] Yan Y., Liao J., Li H., Feng K., Wang H., Wang R., Li S., Ji S., *International Journal of Electrochemical Science*, **2016**, *11*, 226
[36] Kantürk F. A., Coşkuner B., *International Journal of Hydrogen Energy*, **2013**, 38, 2824
[37] Meşe E., Kantürk F. A., Filiz C. B., *Applied Clay Science Journal*, **2018**, *153*, 95
[38] Andrieux J., Demirci U. B., Miele P., *Catal. Today*, **2011**, *170*(1), 13
[39] Yun R., Ma W., Wang S., Jia W., Zheng B., *Inorg. Chem.*, **2019**, *58*(9), 6137
[40] Kumar V., Roy B., Sharma P., *Int. J. Hydrogen Energy*, **2019**, *44*, 22022
[41] Yan J., Liao J., Li H., Wang H., Wang R., *Catalysis Communications*, **2016**, *84*, 124
[42] Meşe E., Kantürk F. A., Coşkuner F. B., Pişkin S., *Appl. Clay Sci.*, **2018**, *153*, 95
[43] Patel N., Fernandes R., Guella G., Miotello A., *Appl. Catal. B Environ.,* **2010**, *95*(1/2), 137
[44] Wang Y., Meng W., Wang D., Li G., Wu S., Cao Z., Zhang K., Wu C., Liu S., *Int. J. Hydrogen Energy*, **2017**, *42*(52), 30718
[45] Li C., Wang D., Wang Y., Li G., Hu G., Wu S., Cao Z., Zhang K., *J. Colloid Interface Sci.*, **2018**, *524*, 25
[46] Yin Y., Xiang C., Chu H., Zhang H., Fen X., Yan E., Sun L., Tang C., Zou Y., *Appl. Surf. Sci.*, **2018**, *460*, 25
[47] Wei Y., Wang R., Meng L., Wang Y., Li G., Xin S., Zhao X., Zhang K., *Int. J. Hydrogen Energy*, **2017**, *42*(15), 9945
[48] Izgi M. S., Şahin Ö., Saka C., *Int. J. Hydrogen Energy*, **2016**, *41*(3), 1600
[49] Chang J., Tian H., Du F. *Int. J. Hydrogen Energy*, **2014**, *39*(25), 13087
[50] Vernekar A. A., Bugde S. T., Tilve S., *Int. J. Hydrogen Energy*, **2012**, *37*, 327
[51] Wang Y., Wang D., Zhao C., Meng W., Zhao T., Cao Z., Zhang K., Bai S., Li G., *Int. J. Hydrogen Energy*, **2019**, *44*(21), 10508
[52] Zhao Y., Ning Z., Tian J., Wang H., Liang X., Nie S., Yu Y., Li X., *J. Power Sources*, **2012**, *207*, 120
[53] [Liang Y., Wang P., Dai H. B., *J. Alloys Compd.*, **2010**, *491*(1/2), 359
[54] Loghmani M. H., Shojaei A. F., *Energy*, **2014**, *68*, 152
[55] Tian H., Guo Q., Xu D., *J. Power Sources*, **2010**, *195*(8), 2136